Journal of
Nanoscience and Nanotechnology
Vol. 20, 4648–4651, 2020
www.aspbs.com/jnn

Electrical Characteristics of Molecular Junctions Fabricated by Inverted Self-Assembled Monolayer Method

Wang-Taek Hwang, Yeonsik Jang, Minwoo Song, and Takhee Lee*

Department of Physics and Astronomy, Seoul National University, Seoul, 08826, Korea

In this study, we demonstrated the molecular ensemble junctions fabricated by the inverted self-assembled monolayer (iSAM) method in which the molecular layer was deposited on the top electrode surface. The alkyl thiolate molecules were used to benchmark this method and we found that the electrical characteristics of these molecular junctions were comparable to the results reported previously by performing statistical analysis. We expect this iSAM method to enable the molecular junctions with bottom electrode of various materials.

Keywords: Molecular Junctions, Self-Assembled Monolayer (SAM), Alkyl Thiolate.

1. INTRODUCTION

The molecular electronics is a research field that studies fabrication and characterization of molecular junctions consisting of single-molecules or molecular assembly sandwiched by two electrical leads. By the number of molecules participating the electronic conduction, the molecular junctions are classified as the single (a few) molecular junctions [1–5], or molecular ensemble junctions [6–10]. Major structure for molecular ensemble junctions is a vertical stack of bottom electrode—molecular layer—top electrode and the self-assembly is a widely used method to form the molecular layer on the surface of bottom electrode by utilizing the self-bonding nature of particular moiety of the molecules.

Directly depositing another metal film, however, can damage the self-assembled monolayer (SAM) and make the most molecular junction electrically shorted [11]. Therefore, several methods such as inserting interlayer (for example conducting polymer [12, 13] or multi-layer graphene [14–16]) or transferring the top electrode already formed [17] have been introduced to increase the yield of molecular junctions. By these fabrication methods, high-yield molecular junctions were achieved but there still exists limitation in materials for bottom electrodes. For example, thiolates can be self-assembled on only a few kinds of metal such as gold or silver [18, 19].

In this study, we suggest an inverted self-assembled monolayer (iSAM) method to overcome such limitation. The alkyl thiolate SAM is formed on the top electrode and this stack is transferred to the pre-made via-hole structure [13–17] (the structure in which bottom electrode is exposed through a hole by etching the insulating layer). We demonstrate that the current density of molecular junctions and junction yield are comparable to the previous research results. This method enables the materials such as graphene or indium tin oxide (ITO) to be adapted for the bottom electrode in molecular junctions.

2. EXPERIMENTAL DETAILS

2.1. Device Fabrication Process

Figures 1(a)–(d) illustrate the fabrication process of iSAM molecular devices. This process is divided into the fabrication of upper part and lower part of the device. For making the upper part, gold top electrodes (Au^{TOP} 30 nm thick) were deposited on *p*-type (100) Si substrate with 270 nm thick SiO_2 surface by e-beam evaporation with shadow masks. Then, poly(methyl methacrylate) (PMMA) (5% in anisole) was spin-coated (4000 rpm, 60 sec) and annealed at 200 °C. To detach the PMMA/Au^{TOP} stack from the substrate, the sample was immersed in potassium hydroxide (KOH) solution (~25%, 50 °C) for 30 min (Fig. 1(a)). As SiO_2 underneath PMMA or Au^{TOP} was etched by KOH, the PMMA/Au^{TOP} stack could be detached from the substrate. This stack remained in the form of film without winkles or folding because of the support of the punched tape applied before the immersion. This film was rinsed several

*Author to whom correspondence should be addressed.

1533-4880/2020/20/4648/004 doi:10.1166/jnn.2020.17850

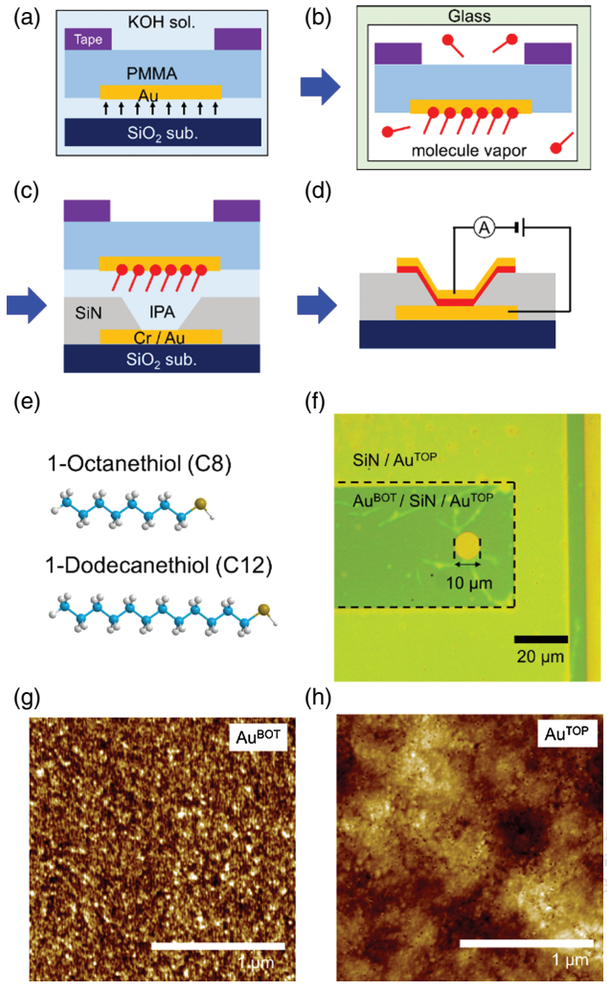

Figure 1. (a–d) Fabrication processes of iSAM molecular junctions. (e) Molecular structure of octanethiol (C8) and dodecanethiol (C12). (f) Optical image (top view) of molecular junction. Surface morphology (AFM images) of (g) bottom electrode and (h) top electrode.

times with deionized water and dried in N_2 stream very carefully.

The molecules deposited on the Au^{TOP} were octanethiol ($CH_3(CH_2)_7SH$, denoted as C8) and dodecanethiol ($CH_3(CH_2)_{11}SH$, denoted as C12) (Fig. 1(e)) widely used for benchmarking the molecular junctions. Since organic solvents such as ethanol or toluene deform or dissolve the thin PMMA film, the method immersing the sample into the molecular solution could not be applied to this study. Instead, we used vapor-phase deposition method [20] for formation of SAM on the Au^{TOP}. The PMMA/Au^{TOP} stack was moved into a vial in which a few drops of molecular liquid were included. While the sealed vial was on the hot plate (75 °C, 4 hours) the molecules were evaporated and SAM was formed on the gold surface because of the chemical bonding between thiol moiety (–SH) and gold [19] (Fig. 1(b)). SAM deposition process was performed in the glove box of N_2 environment in which the O_2 and H_2O concentration were both under 1.0 ppm.

To fabricate the lower part of iSAM molecular junction, bottom electrode (Au^{BOT}) of Au 50 nm with Cr adhesive layer was made by sputtering and lift-off method. Then, 100 nm thick silicon nitride (SiN_x) was deposited by the plasma-enhanced chemical vapor deposition (PECVD) method and diameter 10 μm circular hole was created by photo-lithography and wet etching process. Au^{BOT} was exposed through this hole and remaining SiN_x blocked unintended current flow between Au^{TOP} and Au^{BOT}. Finally, the upper part and lower part of the junctions were aligned and attached (Fig. 1(c)). A few drops of isopropanol (IPA) was added before transferring the PMMA/Au^{TOP} stack because the capillary action during vaporization of IPA facilitates the fine contact between two electrodes. The remaining PMMA film was removed by acetone. Figures 1(d) and (f) present the schematic illustration and optical microscopy image of the iSAM molecular device, respectively.

2.2. Measurement

We measured the electrical characteristics of the iSAM devices with a semiconductor parameter analyzer (Keithley 4200 SCS) and a probe station (M5VC, MS tech) in room temperature and ambient condition. Bias voltage was applied to the Au^{BOT} while Au^{TOP} was grounded. The bias voltage was ranged from −1 V to 1 V. Since the surface roughness of electrode affects the formation of SAM and electric properties of molecular junction, we investigated the morphologies of both electrodes with atomic force microscopy (AFM) (NX-10, Park Systems). As described in AFM images (Figs. 1(g and h)), Au^{BOT} shows rougher surface than Au^{TOP}.

3. RESULTS AND DISCUSSION

To characterize the electric properties of iSAM molecular junctions with C8 and C12, we statistically analyzed the data obtained from the electric measurement. The detail information for the number of devices is summarized in Table I. Total device yield (∼29.6%) is less than that of the result from the previous study based on the direct metal transferring method [17] due to the high fabrication failure rate (∼37.0%).

There were two major fabrication failure cases; (1) In the step of SAM formation on Au^{TOP}, the PMMA film was slightly deformed by alkyl thiol molecules and several

Table I. The summary of the statistical analysis.

Molecules	# of junctions	Fabrication failure	Working devices	Shorted	Open
C8 (%)	135 (100)	15 (11.1)	52 (38.5)	47 (34.8)	21 (15.6)
C12 (%)	135 (100)	85 (63.0)	28 (20.7)	5 (3.7)	17 (12.6)
Total (%)	270 (100)	100 (37.0)	80 (29.6)	52 (19.2)	38 (14.1)

winkles remained in the Au^{TOP} film after finishing this step. Poor contact regions in the top electrode was made by these winkles and they were torn out when removing the PMMA. (2) Even there was no winkle in the top electrode, Au^{TOP} films were often detached from the SiN_x surface due to their poor adhesion. The contact of Au^{TOP} to SiN_x surface was crucial to determine de device yield because 15 junctions shared one common top electrode.

Figure 2 presents the results from statistical analysis of the current density versus bias voltage (J–V) data of working molecular devices. As shown in the Figure 2(a), the mean current density of C8 devices is almost two orders of magnitude larger than that of C12 devices and the error bars express the standard deviation of the current density at each voltage step. Representative non-linear shapes of J–V graphs of C8 and C12 junctions are also shown in Figure 2(b). Figure 2(c) is a histogram of the current density in the order or magnitude at 1 V measured from working devices.

Although the mean values of current density for each type of the molecular junctions are in the range of the results reported previously, the large deviations were found. This broad distribution might originate from the defects on surfaces of each electrodes [21] or not uniform contacts between Au^{TOP} and Au^{BOT}. The surfaces of both electrodes consist of small grains, as shown in AFM images (Figs. 1(g and h)). In other words, there are numerous grain boundaries which act as defects during formation of molecular layer. Mechanical defects were also induced when detaching and transferring the top electrode. Top electrodes with tiny winkles also broadened the distribution of current density. The gap caused by winkles in Au^{TOP} made uncertain contact area between two electrodes.

According to many studies in molecular electronics, off-resonant tunneling is known as the major conduction mechanism in the alkanethiolates junctions [22, 23]. The current density decaying exponentially by the molecular length (i.e., $J = J_0 \exp(-\beta d)$ where β is the decay coefficient and d is molecular length) is an evidence that shows the current flows through the molecular wires in the junction. Figure 3 displays $\ln(J)$ versus the number of carbons in the molecules at given bias voltage ranged from 0.2 V to 1.0 V in the step of 0.2 V. The value of β was obtained from the slope of linearly fitted lines at each bias voltages

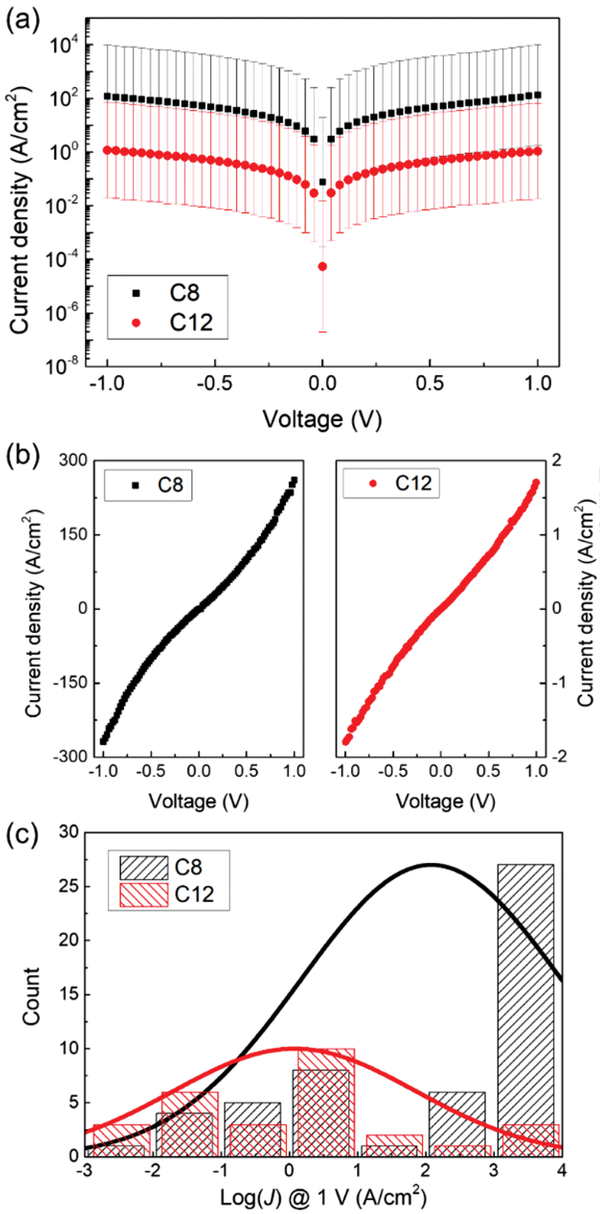

Figure 2. (a) Semi-log plot of statistical J–V data for C8 and C12 devices. (b) Typical non-linear J–V characteristics for molecular junction. (c) Histogram for the order of magnitude of the current density at 1 V for working devices.

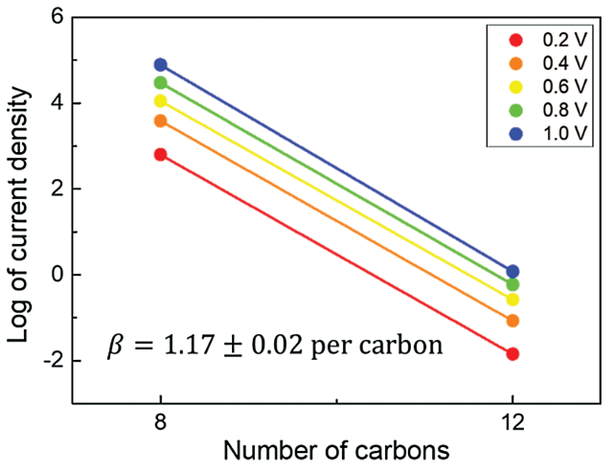

Figure 3. Plot of $\ln(J)$ as a function for the number of carbons at different bias voltages. The values of decay coefficient β (~1.17 per carbon) are extracted from the slopes of the exponentially fitted lines (solid lines).

from Figure 3. We determined the average value of β as 1.17 per carbon or 0.92 $Å^{-1}$ (molecular length of C8 and C12 are 13.2 Å, 18.3 Å which are calculated from Chem-Draw.). The β value we obtained is in agreement with the results previously reported.

4. CONCLUSION

In this study, we fabricated molecular devices with alkanethiolates using inverted self-assembly monolayer (iSAM) method and characterized their electrical properties. Molecular layer is self-assembled on the top electrode in contrast to the conventional molecular ensemble junctions made in the form of via-hole structure with SAM deposited on the bottom electrodes. Electrical characteristics of iSAM devices including average current level and decay coefficient is consistent with the references but suppressing fabrication failure and controlling the defects in junctions are remaining challenges to improve device yield. In the platform of molecular junctions we investigated, alternative materials for bottom electrodes are adaptable. Therefore, we expect that functional molecular devices with various bottom electrode such as graphene or indium tin oxide can be developed by iSAM method.

Acknowledgment: This work was supported by the National Creative Research Laboratory program (grant No. 2012026372) through the National Research Foundation of Korea funded by the Korean Ministry of Science and ICT.

References and Notes

1. Xu, B. and Tao, N.J., **2003**. Measurement of single-molecule resistance by repeated formation of molecular junctions. *Science*, *301*(5637), pp.1221–1223.
2. Reed, M., Zhou, C., Muller, C., Burgin, T. and Tour, J., **1997**. Conductance of a molecular junction. *Science*, *278*(5336), pp.252–254.
3. Park, J., Pasupathy, A.N., Goldsmith, J.I., Chang, C., Yaish, Y., Petta, J.R., Rinkoski, M., Sethna, J.P., Abruña, H.D., McEuen P.L. and Ralph, D.C., **2002**. Coulomb blockade and the Kondo effect in single-atom transistors. *Nature*, *417*(6890), pp.722–725.
4. Song, H., Kim, Y., Jang, Y., Jeong, H., Reed, M.A. and Lee, T., **2009**. Observation of molecular orbital gating. *Nature*, *462*(7276), pp.1039–1043.
5. Xiang, J., Liu, B., Wu, S.-T., Ren, B., Yang, F.-Z., Mao, B.-W., Chow, Y.L. and Tian, Z.-Q., **2005**. A controllable electrochemical fabrication of metallic electrodes with a nanometer/angstrom-sized gap using an electric double layer as feedback. *Angewandte Chemie International Edition*, *44*(8), pp.1265–1268.
6. Haick, H. and Cahen, D., **2008**. Contacting organic molecules by soft methods: Towards molecule-based electronic devices. *Accounts of Chemical Research*, *41*(3), pp.359–366.
7. Chabinyc, M.L., Chen, X., Holmlin, E.R., Jacobs, H., Skulason, H., Frisbie, D.C., Mujica, V., Ratner, M.A., Rampi, M.A. and Whitesides, G.M., **2002**. Molecular rectification in a metal-insulator-metal junction based on self-assembled monolayers. *Journal of the American Chemical Society*, *124*(39), pp.11730–11736.
8. Zhou, C., Deshpande, M., Reed, M., Jones, L. and Tour, J., **1997**. Nanoscale metal/self-assembled monolayer/metal heterostructures. *Applied Physics Letters*, *71*(5), pp.611–613.
9. Loo, Y.-L., Lang, D.V., Rogers, J.A. and Hsu, J.W., **2003**. Electrical contacts to molecular layers by nanotransfer printing. *Nano Letters*, *3*(7), pp.913–917.
10. Kushmerick, J., Naciri, J., Yang, J. and Shashidhar, R., **2003**. Conductance scaling of molecular wires in parallel. *Nano Letters*, *3*(7), pp.897–900.
11. Kim, T.-W., Wang, G., Lee, H. and Lee, T., **2007**. Statistical analysis of electronic properties of alkanethiols in metal-molecule-metal junctions. *Nanotechnology*, *18*(31), p.315204.
12. Akkerman, H.B., Blom, P.W., de Leeuw, D.M. and de Boer, B., **2006**. Towards molecular electronics with large-area molecular junctions. *Nature*, *441*(7089), pp.69–72.
13. Jeong, H., Kim, D., Wang, G., Park, S., Lee, H., Cho, K., Hwang, W.-T., Yoon, M., Jang, Y., Song, H., Xiang, D. and Lee, T., **2014**. Redox-induced asymmetric electrical characteristics of ferrocene-alkanethiolate molecular devices on rigid and flexible substrates. *Advanced Functional Materials*, *24*(17), pp.2472–2480.
14. Wang, G., Kim, Y., Choe, M., Kim, T. and Lee, T., **2011**. A new approach for molecular electronic junctions with a multilayer graphene electrode. *Advanced Materials*, *23*(6), pp.755–760.
15. Koo, J., Jang, Y., Martin, L., Kim, D., Jeong, H., Kang, K., Lee, W., Kim, J., Hwang, W.-T., Xiang, D., Scheer, E., Kabdulov, M., Huhn, T., Pauly F. and Lee, T., **2019**. Unidirectional real-time photo-switching of diarylethene molecular monolayer junctions with multilayer graphene electrodes. *ACS Applied Materials & Interfaces*, *11*(12), pp.11645–11653.
16. Jang, Y., Jeong, H., Kim, D., Hwang, W.-T., Jeong, I., Song, H., Jeong, H., Min, M. and Lee, T., **2016**. Electrical characteristics of benzenedithiol versus methylbenzenthiol self-assembled monolayers in multilayer graphene-electrode molecular junctions. *Journal of Nanoscience and Nanotechnology*, *16*(8), pp.8565–8568.
17. Jeong, H., Kim, D., Kim, P., Cho, M., Hwang, W.-T., Jang, Y., Cho, K., Min, M., Xiang, D., Park, Y., Jeong, H. and Lee, T., **2015**. A new approach for high-yield metal-molecule-metal junctions by direct metal transfer method. *Nanotechnology*, *26*(2), p.025601.
18. Schoenfisch, M.H. and Pemberton, J.E., **1998**. Air stability of alkanethiol self-assembled monolayers on silver and gold surfaces. *Journal of the American Chemical Society*, *120*(18), pp.4502–4513.
19. Poirier, G. and Pylant, E., **1996**. The self-assembly mechanism of alkanethiols on Au(111). *Science*, *272*(5265), pp.1145–1148.
20. Seong, S., Kang, H., Han, S., Sung, T., Park, J.B., Hayashi, T., Hara, M. and Noh, J., **2017**. Formation and structural changes of 4-fluorobenzenethiol self-assembled monolayers on Au(111). *Journal of Nanoscience and Nanotechnology*, *17*(8), pp.5597–5600.
21. Jeong, H., Hwang, W.-T., Kim, P., Kim, D., Jang, Y., Min, M., Xiang, D., Song, H., Park, Y., Jeong, H. and Lee, T., **2015**. Investigation of inelastic electron tunneling spectra of metal-molecule-metal junctions fabricated using direct metal transfer method. *Applied Physics Letters*, *106*(6), p.063110.
22. Wang, W., Lee, T. and Reed, M., **2002**. Mechanism of electron conduction in self-assembled alkanethiol monolayer devices. *Physical Review B*, *68*(3), p.035416.
23. Wang, W., Lee, T. and Reed, M.A., **2004**. Elastic and inelastic electron tunneling in alkane self-assembled monolayers. *The Journal of Physical Chemistry B*, *108*(48), pp.18398–18407.

Received: 29 June 2019. Accepted: 5 August 2019.